Visual Abstract

Elastic surface crack interaction and its engineering critical assessment within the framework of fitness-for-service standards

Gabriel de Castro Coêlho, Antonio Almeida Silva, Marco Antonio dos Santos
Federal University of Campina Grande, Brazil
gabrielcastro_c90@hotmail.com, https://orcid.org/0000-0002-4046-6812
antonio.almeida@ufcg.edu.br, https://orcid.org/0000-0002-7130-8542
santos.marco@ufcg.edu.br

ABSTRACT. In real industrial conditions, it's common to witness the interaction of multiple cracks such that their stress fields and crack driving forces are disturbed. For coplanar cracks, a greater hazard is expected because of the amplification phenomenon. FFS standards deal with this by proposing interaction rules and idealizing a combined flaw for the FAD methodology to be used. The goal of this paper is to analyze the effectiveness of this standards methodology considering twin surface semielliptical cracks on a plate under mode *I* loading on the interaction range using FE analyses. Results confirm that the amplification phenomena due to the interaction are higher on the interacting crack tip and progressively higher as the coplanar horizontal distance decreases. The loss of constraint was observed to decrease as the coplanar horizontal distance decreased, but little change was observed regarding its parametric angular position. A higher amplification was found at the coplanar horizontal distance on which crack interaction is to be considered meaningful, which indicates inconsistency regarding the interaction criteria used on FFS standards. To conclude, the engineering critical assessment of the combined flaw proved to be over-conservative as the remaining operational life was observed on the assessment of the interacting flaws.

KEYWORDS. Crack interaction; Stress intensity factor; Failure assessment diagram; BS 7910; API 579/ASME FFS-1.

OPEN ACCESS

Citation: Coêlho, G. C., Silva, A. A., Santos, M. A., Elastic surface crack interaction and its engineering critical assessment within the framework of fitness-for-service standards, Frattura ed Integrità Strutturale, 60 (2022) 134-145.

Received: 25.11.2021
Accepted: 12.01.2022
Online first: 27.01.2022
Published: 01.04.2022

INTRODUCTION

In many industrial situations, it is common to witness the nucleation of multiple cracks nearby each other on structural components. This might arise from several forms such as stress concentration, environmentally assisted cracking (as in stress corrosion cracking, fatigue-corrosion, or hydrogen embrittlement – where branched cracks are possible), or inefficient manufacturing processes, such as multipass welding stacked flaw [1]. Apart from these, multiple cracks might

nucleate, grow, and coalesce under quasi-static as well as cyclic loading. Common examples of industrial components and structures in which cracks nucleate and interact with each other might be found in the aeronautic and process industry, and specifically in the latter, in pressure vessels and piping systems, and their components [2]. Among all, surface cracks are within the most frequently observed type of cracks in these components and structures.
Within the solid mechanics framework, the local stress field, and consequently the crack driving forces are disturbed by the existence of neighboring stress concentration and stress intensification, which are the case of interacting cracks [3]. Within the linear elastic fracture mechanics, an evaluation of the influence of crack interaction can be computed by the interaction factor, such that,

$$\gamma=\frac{K^{int}}{K^{\infty}} \tag{1}$$

where K^{int} and K^{∞} are the stress intensity factors considering a crack interacting with another and the same crack under no interaction, respectively. When $\gamma > 1$ it is said to exist an amplification, which simply means that the stress field ahead of the crack front was magnified by a neighboring crack. On the other hand, when $\gamma < 1$, it simply implies that the stress field ahead the crack front diminishes due to the neighboring crack in a so-called shielding. It is known that coplanar interacting cracks induce the amplification on each other, while cracks located at parallel plans induce shielding. In this sense, only coplanar cracks are considered structural hazards. This was the main conclusion of Moussa et al. [2], that have analyzed the effect of the interaction of semi-elliptical surface cracks at a plate considering the parametric angular position, Φ, at the interaction tip (Φ = 180°), the opposite tip (Φ = 0°) and the deepest tip (Φ = 90°) considering a coplanar horizontal distance, *s*, and a parallel vertical distance, *h*, between the cracks. Similar conclusions were obtained by Coules [4] in comparison to the results of Yoshimura et al. [5] for two coplanar surface semielliptical cracks separated by a horizontal distance, both showing that amplification at the interaction crack tip is assisted by the decrease of the distance between them, while little or no amplification is verified in the other parametric angular positions.
Crack interaction may also be influenced by cracks dimensions, highlighted in terms of the aspect (a/c) and depth ratios (a/B), where a, c and B are defined in Fig. 1(a) and Fig. 1(c). Azuma et al [6] have investigated the influence of both ratios for surface coplanar semielliptical cracks in a mode I loading, and have concluded that amplification is more pronounced for lower aspect ratios and higher depth ratios. These were confirmed by Bezensek and Coules [7] for a pair of twin surface cracks.
Be as it may, the current assessment methodology considered by worldwide known fitness-for-service (FFS) standards BS 7910 [8] and API 579/ASME FFS-1 [9] is based on defining an effective crack (combined flaw), whose dimensions are based on the real interacting cracks dimensions. The main goal of this approach is to avoid a non-conservative scenario where cracks local driving force is significantly higher than the value used in the assessment if those cracks were standalone or out of interaction range [1]. According to BS 7910 [8], the coplanar horizontal distance between two semielliptical surface cracks for interaction, s, is such that,

$$s \le \max\left(\frac{1}{2}a_1;\frac{1}{2}a_2\right), \text{if } \frac{a_1}{c_1} \text{ or } \frac{a_2}{c_2}<1 \tag{2}$$

or,

$$s \le 2c_1, \text{if} \frac{a_1}{c_1} \text{ and } \frac{a_2}{c_2}>1 \tag{3}$$

for $c_1 < c_2$, and for API 579/ASME FFS-1 [9], Eqn.(2) is valid for every aspect ratio. In both standards, the effective flaw dimensions are such that,

$$a = \max(a_1;a_2) \tag{4}$$

and,

$$2c = 2c_1 + 2c_2 + s \tag{5}$$

and these equations are based on a 10% amplification after the results pointed by Bezensek and Hancock [10], which evaluated the previous 20% amplification used since PD 6493 [11] (predecessor of BS 7910) to be extremely conservative. After determining the effective crack dimensions, the assessment can proceed using, for example, the failure assessment diagram (FAD).

The main goal of the current study is to investigate the limits of using combined flaws considering the mentioned interaction rules on the FAD methodology in comparison to the interaction phenomena problem within the linear elastic fracture mechanics framework.

METHODOLOGY

For the current investigation on crack interaction, several finite element simulations were executed considering a pair of twin cracks on a structural steel plate under mode *I* loading, as shown in Fig. 2(b), with Young's modulus E = 210 GPa and Poisson's ratio ν = 0.3. The choice of studying twin cracks aims to observe only the effect of the coplanar distance, keeping the effects of aspect and depth ratio constants. The cracks dimensions, as shown in Fig. 2(c), were defined such that $a/B = 0.5$ and $a/c = 0.5$. As the considered plate was set to have B = 25 mm, crack dimensions are a = 12.5 mm and c = 25 mm. Raju and Newman [12] have stated that to minimize the effect of a hollow cylinder length (L) on the stress intensity factor of a superficial crack contained in it, the finite element model should have $L/c \geq 10$. Considering the same criteria, the minimum plate width dimension was set as,

$$\frac{W}{c_1 + c_2 + s^{max}} \geq 10 \tag{6}$$

where s^{max} is the maximum interaction coplanar distance according to Eqn.(2) and Eqn.(3), which brings about W = 564 mm. The plate height $2H$ was considered equal to the plate width.

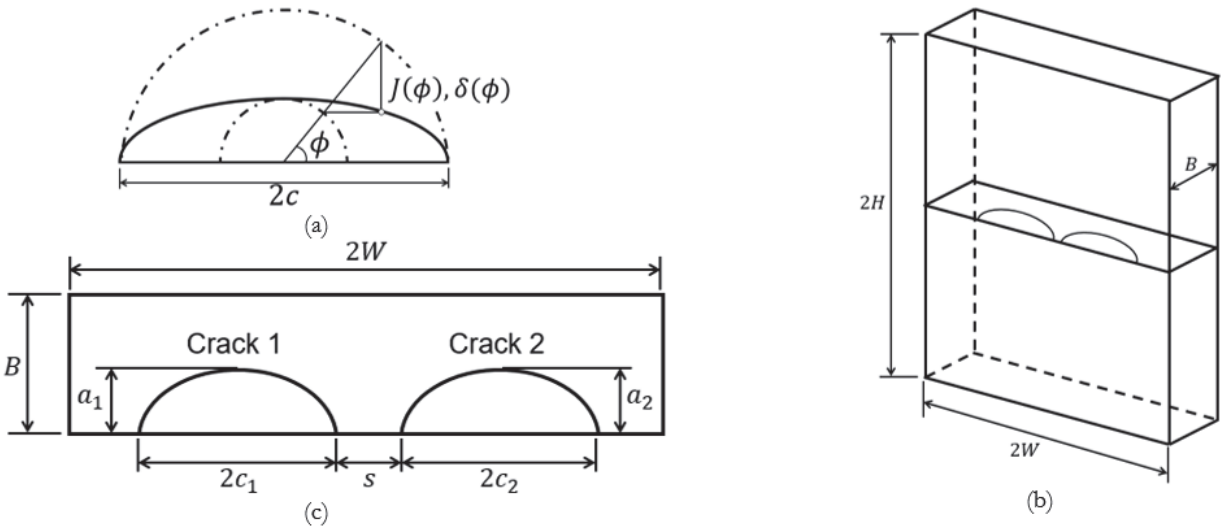

Figure 1: (a) Semi elliptical stress intensity factor profile along with parametric angular position; (b) Coplanar interaction schematic and cracks dimensions; (c) Plate with pair of twin surface cracks.

The horizontal coplanar distance was ranged from out of the interaction criteria dimension according to Eqn.(2) and Eqn.(3) to a minimum value of $s/(c_1 + c_2) = 0.1$. For each value of s, the stress intensity factor semi-elliptical profile was extracted and plotted along with the parametric angular position, according to Fig. 2(a). To verify in which direction crack propagation due to interaction would occur, the T-stress profile was also extracted. T-stress (T) is the second finite term of the Williams

solution to the stress field near a crack tip on an elastic body [3], and their relation to the stress intensity factor is evaluated by the biaxiality ratio,

$$\beta=\frac{T\sqrt{\pi a}}{K_I} \tag{7}$$

whose usage is a qualitative indicator of the crack tip constraint such that higher values indicate high triaxiality stress fields and lower values indicate loss of crack tip constraint. Crack propagation, of course, would occur under high triaxiality levels.

RESULTS AND DISCUSSION

Finite Element Modelling for Surface Interacting Cracks

All crack interaction simulations were performed in ABAQUS®. The model, as shown in Fig. 2(a), consists of a one-quarter plate (with symmetry boundary conditions applied on the symmetry planes) of a master instance with a coarser mesh and a slave instance with a finer mesh. Both instances are attached using tie constraint, which imposes all nodes displacements on the slave surfaces equal to the displacements of the nodes on the slave surfaces. The crack front on the slave instance is shown in Fig. 2(b). The mesh around the semi-elliptical crack front is a typical spider mesh, shown in Fig. 2(c), where the first inner ring elements consist of tridimensional fully integrated 6-node linear wedge elements (C3D6) and the elements of the outer rings consist of tridimensional fully integrated 8-node linear brick elements (C3D8). The rest of the slave and master instances consist of C3D8 elements. The number of degrees of freedom on each model varied according to the $s/2$ distance, which affects the meshing algorithm on the slave instance.

As there is no analytical or experimental solution for the stress intensity factor or T-stress semielliptical profile for interacting cracks, the model described above was compared with the results of Coules [4] and Yoshimura et al. [5]. Both studies derived the elastic interaction factor γ along with the parametric angular position Φ/π. The results of the present study with the same crack dimensions configuration and their results are compared in Fig. 3(a). It is possible to see that the present results are in good agreement with the results of the cited authors with a maximum error of 3.99 % considering the interacting parametric angular position ($\Phi/\pi = 0$) regarding the latter, which is enough to validate the efficiency of the described model. Additionally, an standalone and combined flaw (with dimensions according to Eqn.(4) and Eqn.(5)) crack models were constructed and their stress intensity factor profile solutions compared to the analytical solution given by BS 7910 [8] (which was assessed and considered accurate for the aspect and depth ratios considered [13]) and good agreement is also observed just as seen in Fig. 3(b).

Effect of crack interaction on Stress Intensity Factor and T-stress Profile

Considering the interaction of the twin cracks, several finite element models were simulated varying the coplanar horizontal distance between the cracks such that $s/(c_1 + c_2)$ = 0.2;0.18;0.16;0.14;0.13;0.125;0.12;0.11;0.10. For every model, the stress intensity factor profile (normalized by the magnitude $\sigma\sqrt{(\pi a)}$, where σ is the remote tensile stress) and biaxiality ratio profile along the normalized parametric angular position has been extracted and are both shown in Fig. 4(a) and Fig. 4(b), respectively. In Fig. 4(a), the standalone and combined flaw stress intensity factor profile and, in Fig. 4(b), biaxiality ratio profiles, both obtained by their finite element model, are also shown for comparison. Considering the interaction rule considered by BS 7910 [8] and API 579/ASME FFS-1 [9] for the twin surface cracks, according to Eqn.(2) and Eqn.(3), the interaction should be only relevant when $s/(c_1 + c_2) = 0.125$.

For the stress intensity factor, it is possible to see that the interaction affects the magnitude of the whole profile due to the amplification phenomena in comparison the standalone crack profile and the highest amplification is located on the interacting parametric angular position, that is, $\Phi/\pi = 0$ ($\Phi = 0°$). Further, as closely as the coplanar cracks are located, the higher is the amplification phenomena. This is by what was observed by Yoshimura et al. [5]; Moussa et al. [2]; and Coules [4]. Also worth mentioning that the combined flaw induces a much higher stress intensity factor magnitude than the smallest coplanar horizontal distance interacting case here considered, which is in accordance with the current methodology of both BS 7910 [8] and API 579/ASME FFS-1 [9], although the maximum magnitude is located at $\Phi/\pi = 0.5$ ($\Phi = 90°$)

For the biaxiality ratio, it is noticeable that the combined flaw induces a much higher constraint with maximum magnitude at $\Phi/\pi = 0.15833$ ($\Phi = 28.5°$) and $\Phi/\pi = 0.84167$ ($\Phi = 151.5°$), different when compared to the standalone crack, that

exhibits maximum magnitude at $\Phi/\pi = 0.11$ ($\Phi = 19.8°$) and $\Phi/\pi = 0.89$ ($\Phi = 160.2°$). Considering the interaction between the twin cracks, the whole biaxiality ratio profile is affected with greater amplification phenomena located at $\Phi/\pi < 0.3$ ($\Phi < 54°$). The specific parametric angular position indicating the highest constraint location little changes as both cracks tend to proximate each other, lying on the interval $0.05 < \Phi/\pi < 0.07$ ($9° < \Phi < 12.6°$). Tab. 1 summarizes the maximum value of the biaxiality ratio (β^{max}) and its parametric angular position as a function of the coplanar horizontal distance between both cracks.

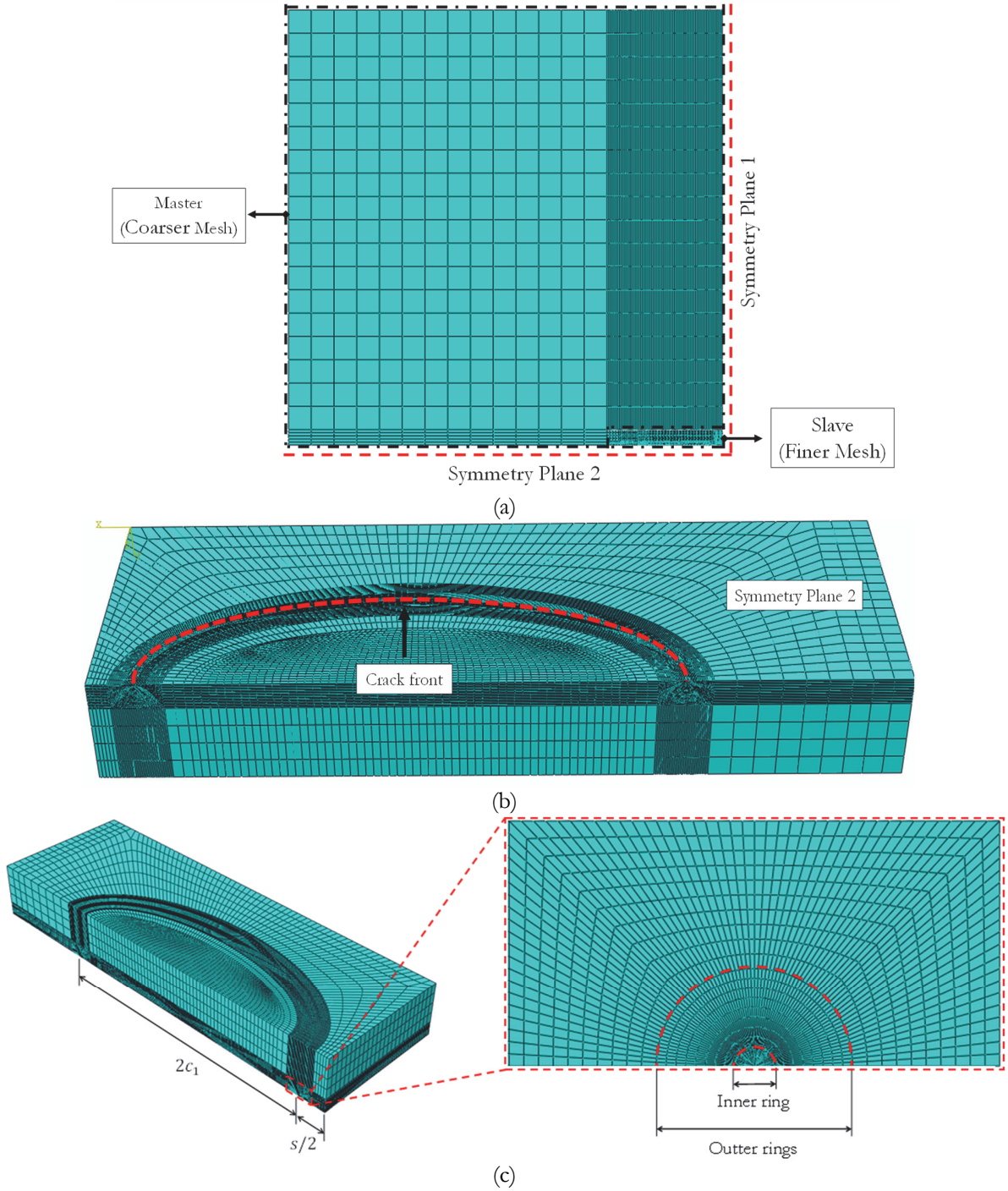

Figure 2: (a) One-quarter plate model with master and slave instances attached with tie constraint; (b) Crack front location on slave instance; (c) Slave instance and spider mesh structure around semielliptical crack front.

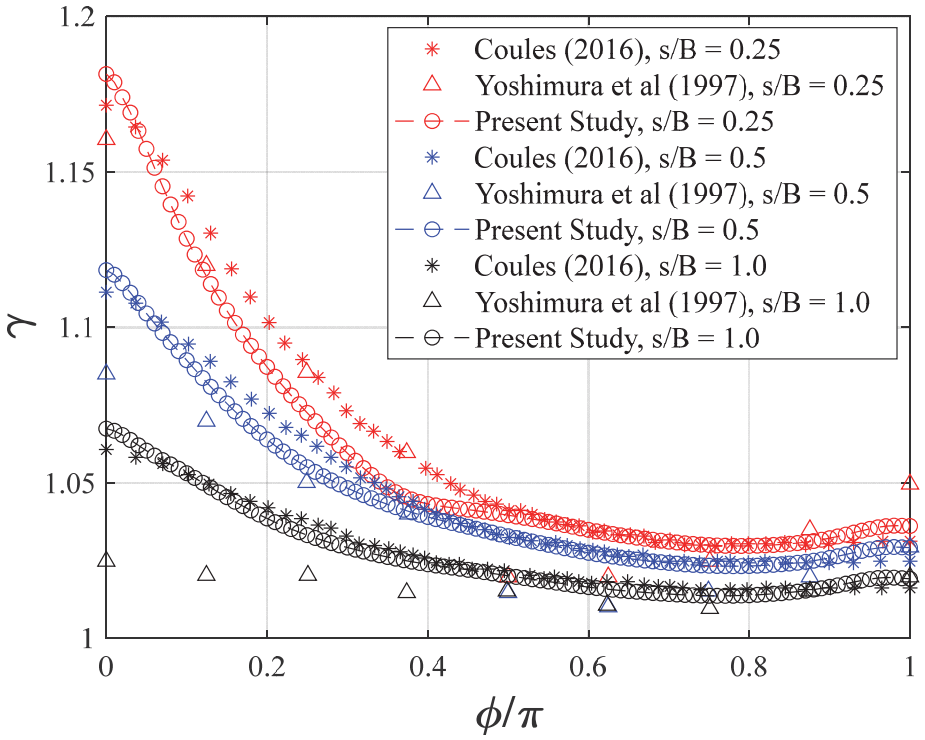

(a)

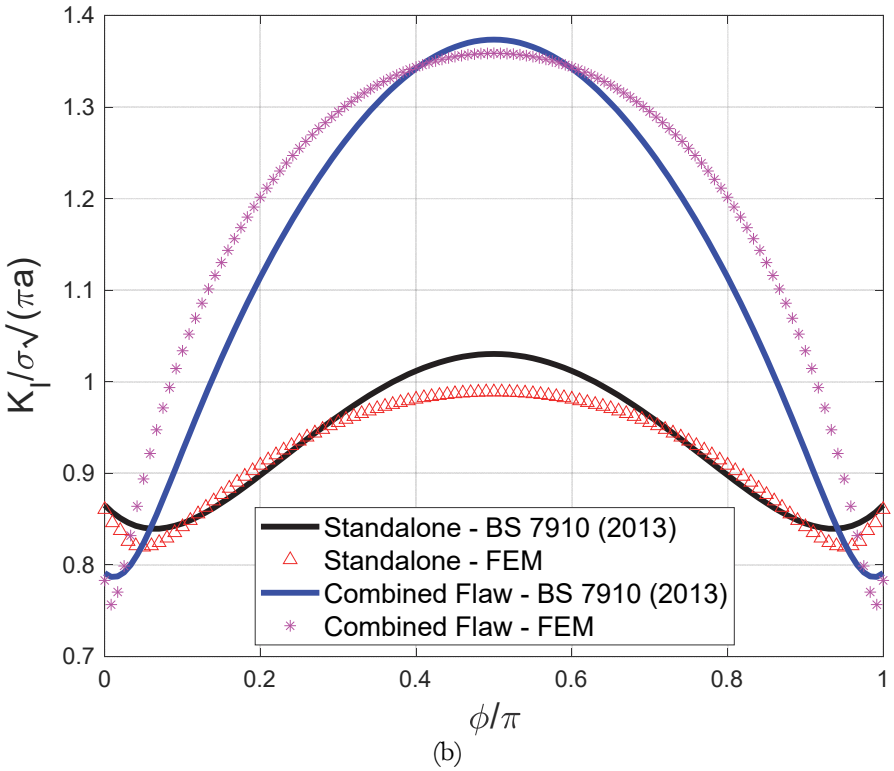

(b)

Figure 3: Comparison of the present model results with (a) Coules [4] and Yoshimura et al. [5]; (b) BS 7910 [8] analytical solution.

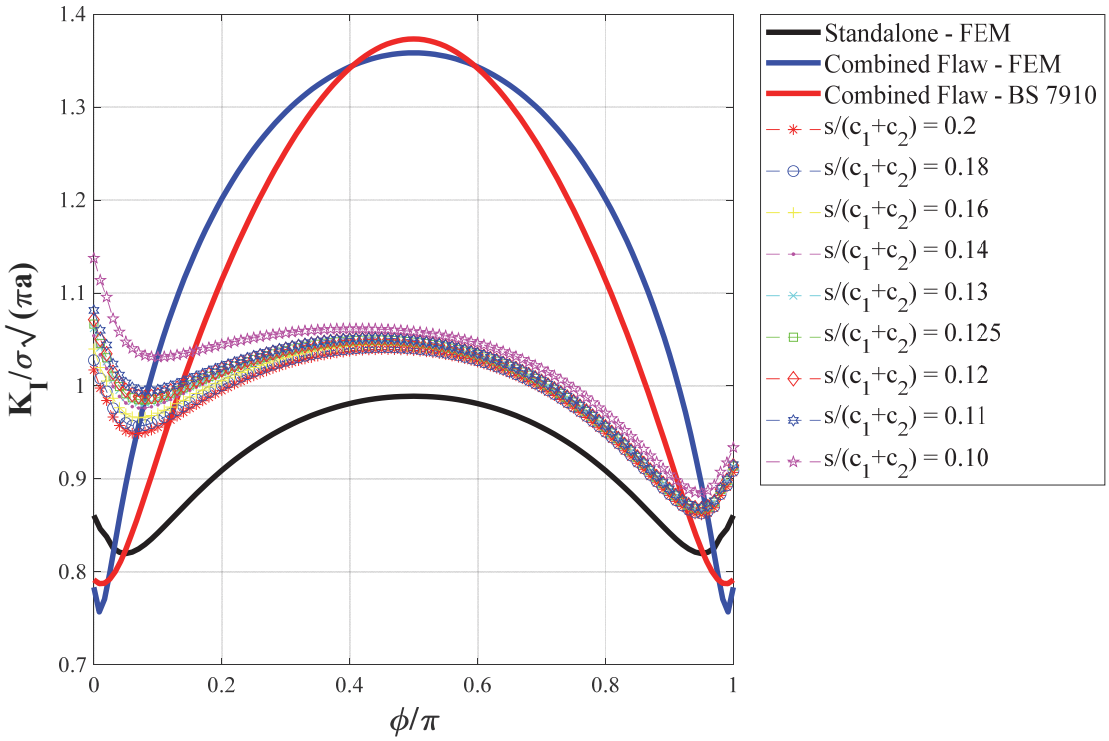

(a)

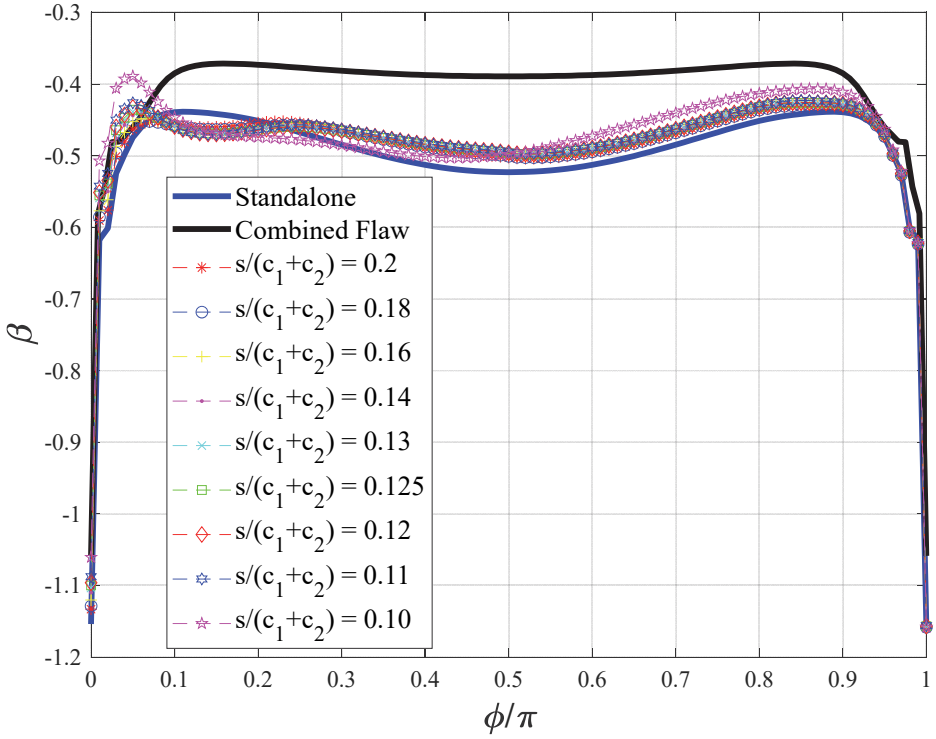

(b)

Figure 4: (a) Stress intensity factor profile for several coplanar horizontal distances; (b) Biaxiality ratio profile for several coplanar horizontal distances.

$s/(c_1 + c_2)$	β^{max}	Φ/π (Φ)
0.2	-0.4534	0.07 (12.6°)
0.18	-0.4522	0.07 (12.6°)
0.16	-0.4484	0.06 (10.8°)
0.14	-0.4420	0.06 (10.8°)
0.13	-0.4383	0.06 (10.8°)
0.125	-0.4358	0.05 (9°)
0.12	-0.4328	0.05 (9°)
0.11	-0.4262	0.05 (9°)
0.10	-0.3892	0.05 (9°)
Standalone	-0.4386	0.11 (19.8°)
Combined Flaw	-0.3715	0.158 (28.5°)

Table 1: Maximum biaxiality ratio magnitudes and their parametric angular position as a function of the coplanar horizontal distance.

Elastic Interaction Factor Analysis

Fig. 5(a) shows the elastic interaction factor profile along with the parametric angular position for the considered coplanar horizontal distances. As expected, the amplification phenomenon is higher as the cracks approximate each other with the highest amplification located at $\Phi/\pi = 0$ ($\Phi = 0°$). Fig. 5(b) shows the elastic interaction factor at $\Phi/\pi = 0$ ($\Phi = 0°$) as a function of the coplanar horizontal distances here considered. According to Eqn.(2), interaction should only be significant and demanding flaw re-characterization as a unique combined flaw for $s/(c_1 + c_2) = 0.125$ (solid black vertical line) or less. For this coplanar horizontal distance, however, an approximate 24% amplification is verified for the twin cracks here considered, which is not in accordance with the 10% amplification prerogative stated by Bezensek and Hancock [10] to reformate the interaction criteria on the current BS 7910 (2013). Besides that, it can also be observed that coplanar horizontal distances higher than $s/(c_1 + c_2) = 0.125$ induced elastic interaction factors higher than 20% amplification (dashed red horizontal line), which was the basis for the interaction criteria before the current BS 7910 [8].

Engineering Critical Assessment

The Failure Assessment Diagram (FAD) is the common assessment methodology used on both BS 7910 [8] and API 579/ASME FFS-1 [9]. For the current study, the basic assessment level will be used as it only requires little information regarding material properties. Still, fracture toughness, yield, and tensile strength values are required so the assessment point is plotted on the FAD. The material properties here used are taken from Hurlston, Sharples and Sherry [14] for an ASTM A533B Class 1 pressure vessel steel at 20 °C and summarized on Tab. 2.

The assessment points are calculated such that:

$$K_r = \frac{K}{K_{mat}} \tag{8}$$

and,

$$L_r = \frac{\sigma_Y}{\sigma_r} \tag{9}$$

where K_{mat} is the materials' fracture toughness; σ_Y is its Yield strength; σ_r is the reference stress regarding the structure and cracks geometry (a compendium can be found on BS 7910 [8] and the single surface crack reference stress was used here).

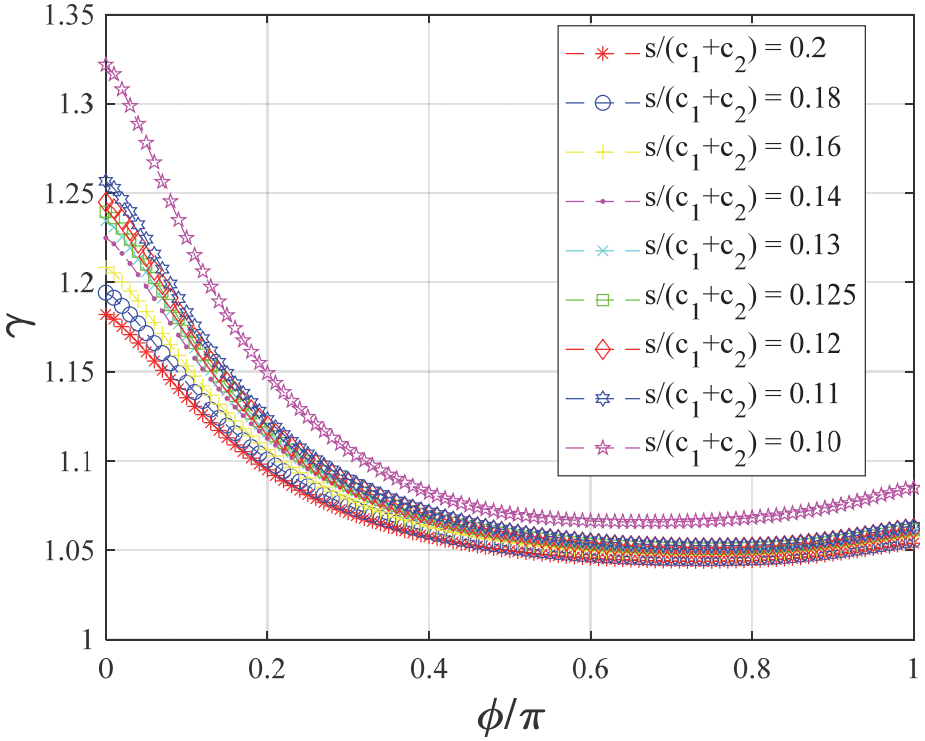

(a)

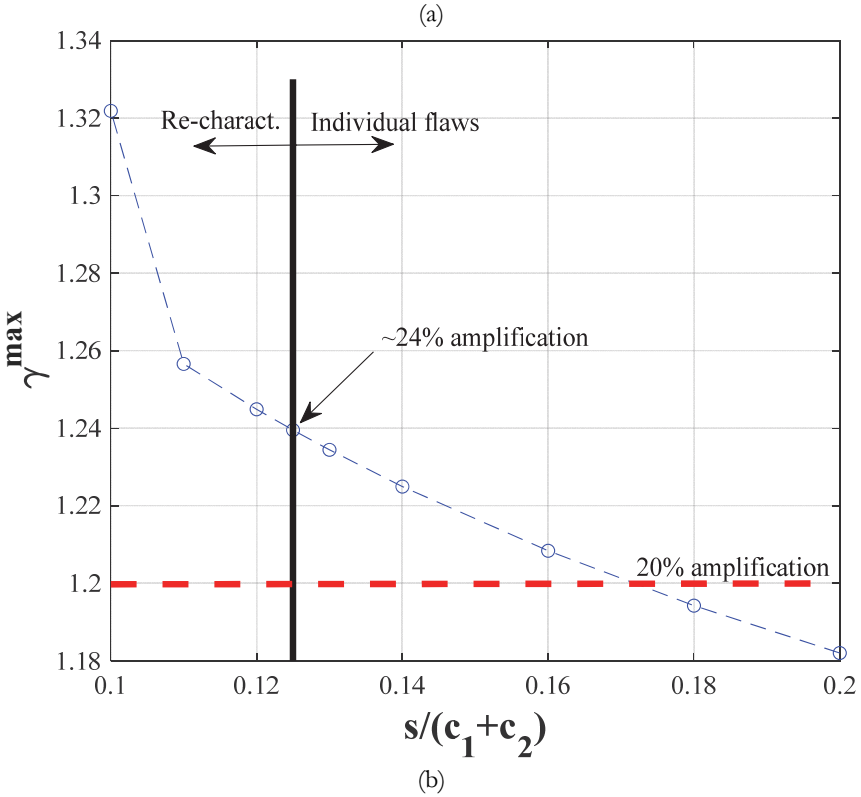

(b)

Figure 5: (a) Elastic interaction factor profile along with the parametric angular position; (b) maximum elastic interaction factor as a function of the coplanar horizontal distance.

Mechanical property	Value [Unit]
Young's modulus	210 [GPa]
Poisson's ratio	0.3 [-]
Yield stress	450 [MPa]
Yield Strength	670 [MPa]
Fracture toughness	90 [MPa√m]

Table 2: Mechanical properties for ASTM A533B Class 1 pressure vessel steel at 20 °C.

Fig. 6 shows two FADs: one for materials that exhibit continuous yielding (blue solid line) and another one for materials that exhibit discontinuous yielding (Lüder's plateau – red solid line). The FAD methodology assures safe operation of the structure with a crack-like flaw as long as the assessment points are below the FAD lines. In Fig. 7, it is observed that if the material exhibits continuous yielding, only the standalone flaw case would be safe for operation. On the other hand, if the material exhibits discontinuous yielding, not only the standalone flaw case but also the interacting flaws cases would operate safely. The combined flaw, however, probably would not operate safely. This difference between the minimum coplanar horizontal distance interacting flaw case (which induces higher amplification) and the FAD line might be interpreted as fully operational life that the structure could have. The combined flaw methodology, however, induces some conservatism on the assessment and would demand the structure to be repaired or discarded.

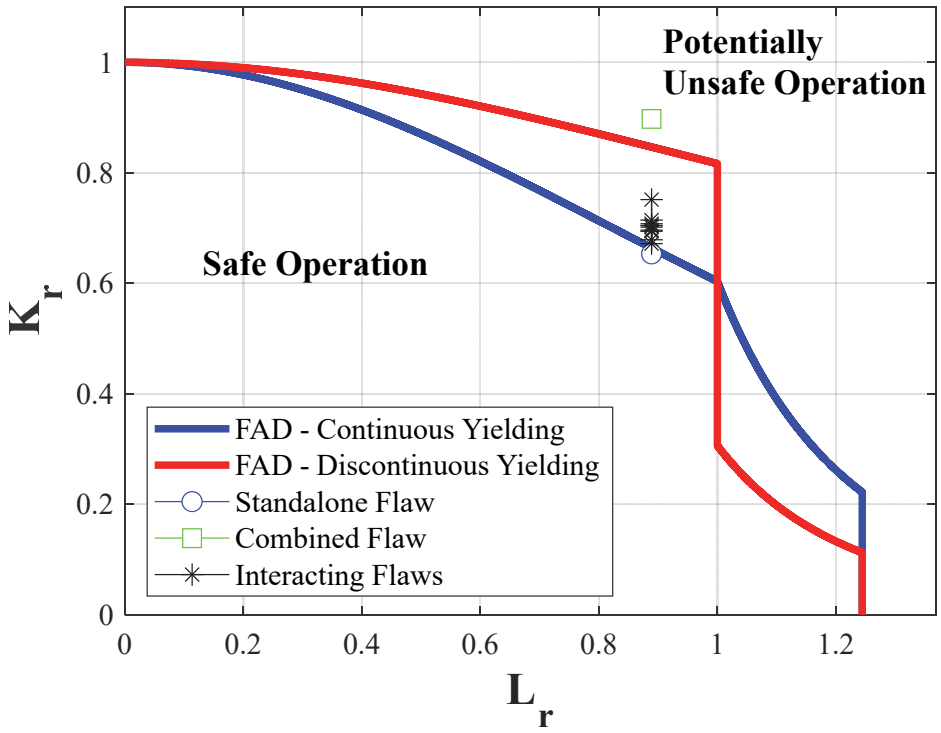

Figure 6: FAD with assessment points.

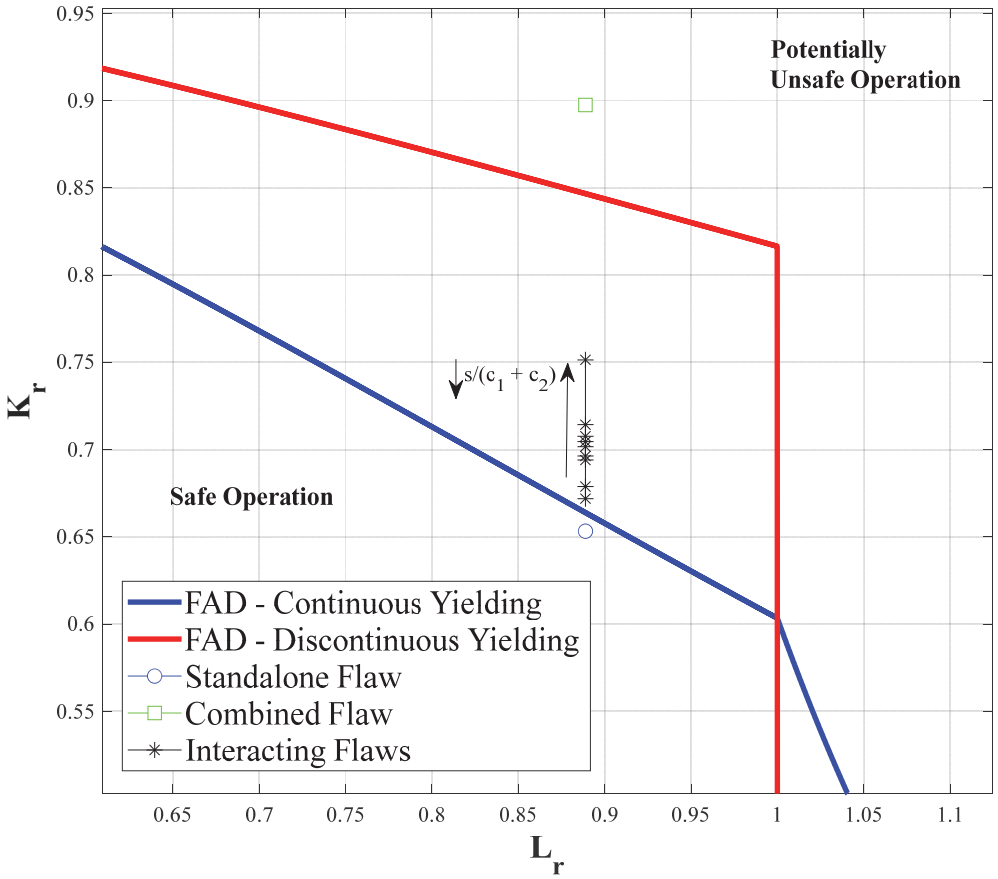

Figure 7: A closer look at assessment points.

Conclusions

The study of interacting twin cracks on a plate under mode *I* loading has been performed. It can be seen that the finite element models developed are representative of stress intensity factor and T-stress profiles when compared to the results of other studies. For the stress intensity factor, it was noticeable that the amplification phenomenon affects its magnitude along with the whole profile, exhibiting higher amplification at the interaction parametric angular position, which is according to what has been observed by other authors. Regarding the biaxiality ratio, it is seen that the smaller the coplanar horizontal distance between the cracks, the higher is the amplification phenomena, but little changing the parametric angular position of the higher constraint.

For the coplanar horizontal distance according to the interaction criterion to which interaction would be considerable, it was observed that the amplification is higher than 10%, which is the basis for crack interaction to be considered meaningful, showing some inconsistency with the criteria used in both BS 7910 [8] and API 579/ASME FFS-1 [9]. Regarding the engineering critical assessment, it was possible to conclude that the combined flaw induces too much conservatism into the assessment, such that for interacting cracks, there would be some safe operational life before repair/discard.

Acknowledgments

The authors would like to acknowledge the Coordination for the Improvement of Higher Education (CAPES) and the National Council for Scientific and Technological Development (CNPq, under grant Universal Research Proc. 408131/2018–7) for funding this research.

REFERENCES

[1] Bezensek, B. and Sharples, J. (2018). Flaw interaction rules given in BS 7910:2013 - The history and the way forward, International Journal of Pressure Vessels and Piping, 168, pp. 225-232. DOI: 10.1115/PVP2018-84119.

[2] Moussa, W. A., Bell, R. and Tan, C. L. (1999). The interaction of two parallel non-coplanar identical surface cracks under tension and bending, International Journal of Pressure Vessels and Piping, 76(3), pp. 135-145. DOI: 10.1016/S0308-0161(98)00125-2.

[3] Anderson, T. L. (2017). Fracture mechanics: fundamentals and applications. 4 ed. Boca Raton: CRC Press. DOI: 10.1201/9781315370293.

[4] Coules, Harry E. (2016). Stress intensity interaction between dissimilar semi-elliptical surface cracks, International Journal of Pressure Vessels and Piping, 146, pp. 55-94. DOI: 10.1016/j.ijpvp.2016.07.011.

[5] Yoshimura, S., Lee, J. S. and Yagawa, G. (1997). Automated system for analyzing stress intensity factors of three-dimensional cracks: its application to analyses of two dissimilar semi-elliptical surface cracks in plate, Journal of Pressure Vessel Technology, 119(1), pp. 18-26. DOI: 10.1115/1.2842261.

[6] Azuma, K., Li, Y. and Hasegawa, K. (2015). Evaluation of stress intensity factor interactions between adjacent flaws with large aspect ratios, ASME 2015 Pressure Vessels and Piping Conference - PVP2015. Boston, USA. 19-23 July. DOI: 10.1115/PVP2015-45063.

[7] Bezensek, B. and Coules, H. E. (2018). Recent studies towards updating the BS7910 flaw interaction rule, ASME Pressure Vessels and Piping Conference, PVP2018, Prague, Czech Republic. 15-20 July. DOI: 10.1115/PVP2018-84119.

[8] BS 7910 (2013). Guide to methods for assessing the acceptability of flaws in metallic structures. London: British Standard Institution.

[9] API 579/ASME FFS-1 (2016). Fitness-for-service. Washington: API Publishing Services.

[10] Bezensek, B. and Hancock, J. W. (2004). The re-characterization of complex defects part I: fatigue and ductile tearing, Engineering Fracture Mechanics, 71(7-8), pp. 981-1000. DOI: 10.1016/S0013-7944(03)00155-3.

[11] PD 6493, 1980. Guidance on some methods for the derivation of acceptance levels for defects in fusion welded joints. London: British Standard Institution.

[12] Raju, I. S. and Newman, J. C. (1982). Stress-intensity factors for internal and external surface cracks in cylindrical vessels. Journal of Pressure Vessel Technology, 104(4), pp. 293–298. DOI: 10.1115/1.3264220.

[13] Coêlho, G. C., Silva, A. A., Santos, M. A., Lima, A. G. B., Santos, N. C. (2019). Stress intensity factor of semielliptical surface crack in internally pressurized hollow cylinder – a comparison between BS 7910 and API 579/ASME FFS-1 solutions, Materials, 12(7), pp.1042-1058. DOI: 10.3390/ma12071042.

[14] Hurlston, R. G., Sharples, J. K., Sherry, A. H. (2015). Understanding and accounting for the effects of residual stresses on cleavage fracture toughness measurements in the transition temperature regime, International Journal of Pressure Vessels and Piping, 128, pp. 69-83. DOI: 10.1016/j.ijpvp.2015.02.001.